

# Comparison of mixing effectiveness of a large-scale static mixer between CFD simulation and image concentration measurement

**Tomas Daubner<sup>1</sup>, Jens Kitzhofer<sup>2</sup>, Mircea Dinulescu<sup>3</sup>**

<sup>1</sup> Weisteinde 10, Voorburg, The Netherlands, [tomas.daubner@apexgroup.eu](mailto:tomas.daubner@apexgroup.eu), Apex Research B.V.

<sup>2</sup> Weisteinde 10, Voorburg, The Netherlands, [jens.kitzhofer@apexgroup.eu](mailto:jens.kitzhofer@apexgroup.eu), Apex Research B.V.

<sup>3</sup> Weisteinde 10, Voorburg, The Netherlands, [mircea.dinulescu@apexgroup.eu](mailto:mircea.dinulescu@apexgroup.eu), Apex Research B.V.

---

**Abstract:** This article compares the effectiveness of mixing of a static mixer for a large-scale air duct by applying CFD simulation and experimental image based measurements. In order to match real physical conditions, the duct is scaled 1:10 to keep the Reynolds number constant between experiment and reality. Reynolds number in these type of applications ranges from  $10^5$  up to  $10^6$ . For the experimental evaluation of image based data, we applied an image analysis routine and calculated the seeding density distribution. To apply proper boundary conditions for the CFD simulation, the velocity profile upstream of the static mixer has been measured by Laser Doppler Anemometry. The effectiveness of mixing is evaluated for both CFD and image data as coefficient of variance CoV.

**Keywords:** mixing, CFD, image based measurement, static mixer, coefficient of variance

## Introduction

Apex Research Laboratory focuses on the improvement of plate type heat exchangers, the effective use of pressure drop in the ductwork and the mixing effectiveness of various industrial processes. In the sake of mixing effectiveness, Apex Research Laboratory has developed an experimental setup for understanding the physical phenomena like the mixing of multiple jets [1]. This paper continues in the discussion about mixing and evaluates the mixing performance of a large-scale gas/gas static mixer (viscosity ratio 1-10) by using CFD and image based concentration measurement. With respect to [2], mixing is defined as the reduction of inhomogeneity in order to achieve a desired process result. The inhomogeneity can be of concentration or temperature, may be local (downstream of injection nozzles) or global (downstream of heat exchangers). Mixing is applied over the entire range of fluid flow regimes. In large scale ducts the Reynolds number usually exceeds 100.000, thus the flow field can be considered as turbulent. The latest motionless mixers for application in turbulent flow rely on vortex generation away from surfaces. In case of local mixing requirements, the advantages of vortex mixers are the low pressure drop and the short length of duct needed to achieve high degree of homogeneity. In case of global mixing requirements, the vortex mixers might need longer mixing lengths to achieve the desired homogeneity. Shorter mixing lengths are possible with the mixers built of structured plate or bars and well-designed inlet injectors. These designs more aggressively direct the flow, using the increased turbulent energy to achieve mixing. Figure 1 shows a typical situation downstream of a plate type heat exchanger. The temperature distribution varies from e.g. 200°C to 300°C. That temperature non-uniformity may remain up to the entrance into downstream equipment and may cause damage because of design at mean temperature, e.g. 250°C. Standard static mixers as mixer blades are not capable of mixing the global temperature gradient efficiently in a short distance. The proposed static mixer overcomes this issue by a tunneling system, which brings fluid from top to bottom and vice versa.

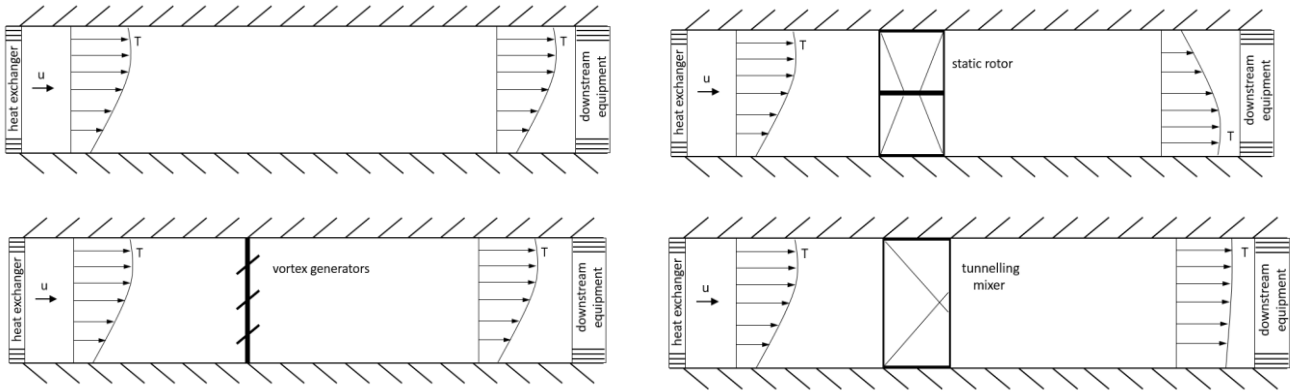


Figure 1 Temperature distribution with global inhomogeneity downstream of the heat exchanger - empty duct (top left), static rotor (top right), vortex generator (bottom left), tunneling static mixer (bottom right)

## Static Mixer

The mixer in this study (Figure 2) consists of triangular bars separated by walls. The mixer can be characterized by four design parameters: number of elements ( $n$ ), angle of triangular bar ( $\alpha$ ), length of triangular bar ( $L$ ) and wall length ( $L_w$ ) (Figure 3). The mixer in this study is defined by  $n=9$ ,  $\alpha=33^\circ$ ,  $L=250$  mm ( $L/D_h=5/6$ ),  $L_w=300$  mm ( $L_w/D_h=1$ ),  $D_h$  is the equivalent diameter of the duct. Additionally, figure 2 shows the flow direction. The flow in the rectangular channel is split into 9 channels separated by thin walls. Due to the asymmetric alternating contractions in the subsequent channels, fluid from top is guided to the bottom and vice versa causing global mixing.

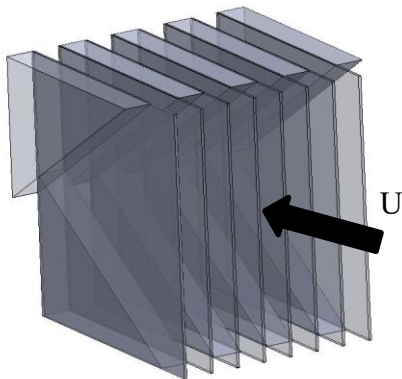


Figure 2 Static Mixer Isometric view

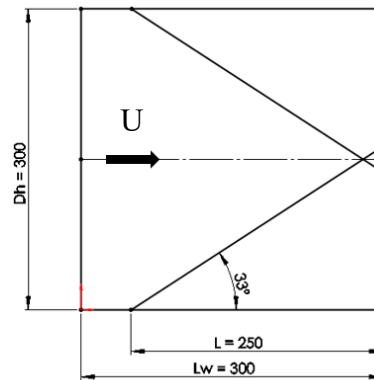


Figure 3 Static Mixer Side view

## Experimental Setup

In order to study the effectiveness of mixing we have constructed an experimental setup shown in Figure 4. The flow is driven by the centrifugal fan MBRC 40/12 M4 0,75kW. The ducting consists of 3 plexiglass ducts (300x300) mm with the lengths (500,1700,1200) mm. A flow conditioner at the inlet of the second duct is used in order to create a uniform velocity distribution in the second duct. The second duct is split by a separation plate. The seeding is injected into the upper part of the second duct (position 700 mm of the second duct), guaranteeing that in the bottom section is no seeding. The static mixer is positioned downstream of the second duct (at the inlet to the third duct). The velocity profile at the position of 1500 mm of second duct is taken by LDA and used in CFD as boundary condition (Figure 5). Figure 6 shows the raw data of image based measurement. CFD results and image based measurement which are taken at the position  $1 \cdot D_h$  and  $2 \cdot D_h$  downstream from the static mixer are presented as normalized concentrations maps.

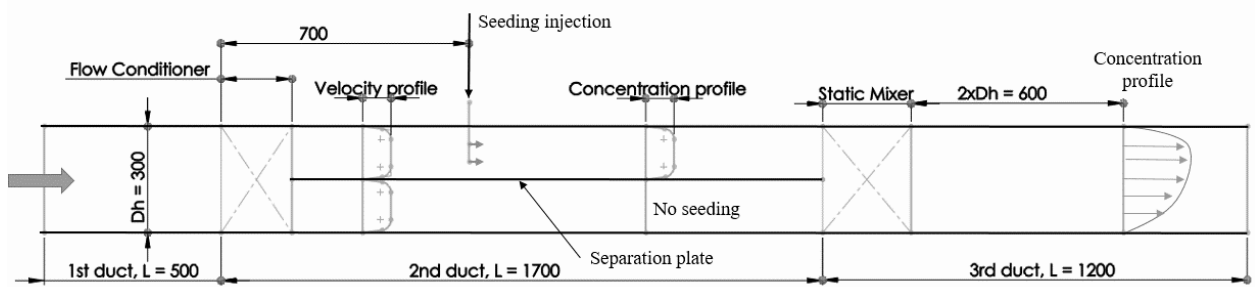


Figure 4 Experimental setup

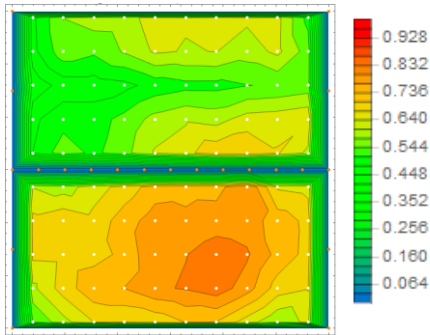


Figure 5 Normalized streamwise velocity profile at position 1500mm of 2nd duct measured with LDA

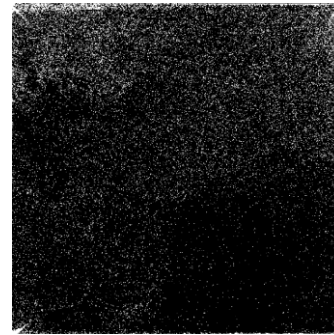


Figure 6 Raw example of image based measurement at position 1\*Dh of 3<sup>rd</sup> empty duct

### Computational Fluid Dynamics simulation - CFD

FLOEFD software has been used (version 17.0.0.) for CFD simulation. To predict turbulent flows, the Favre-averaged Navier-Stokes equations are used. To close the system of equations, FloEFD employs transport equations for the turbulent kinetic energy and its dissipation rate, the so-called realizable k- $\epsilon$  model. [Technical Reference FLOEFD]

In early CFD studies was observed more rapid mixing than experimental studies. This was due to a phenomena called numerical diffusion, when coarse grids numerical rounding errors cause a smoothing of concentration gradients. With finer grids the accuracy of the calculation matches well with the experimental measurements [4].

Mesh independence test has been performed with final amount of 4 million cells with local mesh refinement in the area of static mixer on solid/fluid bordering cells. As inlet boundary condition the measurement of velocity profile with LDA has been used (Figure 5) extended by no-slip condition points in Wolfram Mathematica. The mixing model of FLOEFD is governed by species conservation equations. Figure 7 shows normalized concentration upstream of the static mixer. The concentration maps at the positions 1\*Dh and 2\*Dh downstream from static mixer are shown in Figure 8 and Figure 9.

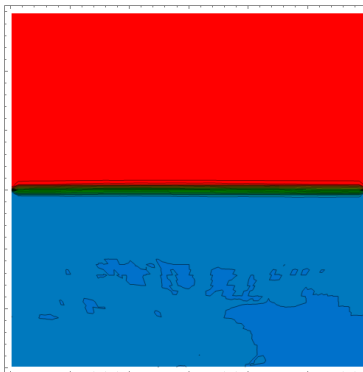


Figure 7 CFD normalized fluid concentration at position 0 mm of the third duct

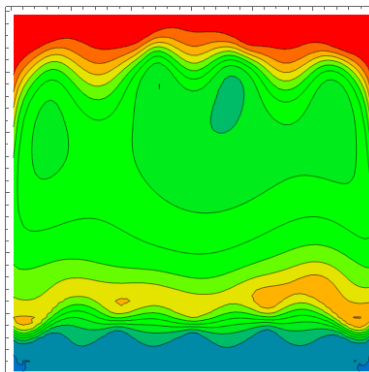


Figure 8 CFD normalized fluid concentration at position 1\*Dh

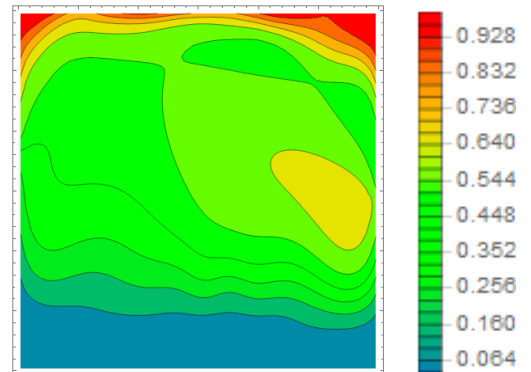


Figure 9 CFD normalized fluid concentration at position 2\*Dh

## Image based measurement

For image based measurement we have used a 4 Mpixel CCD camera, a 145 mJ laser equipped with a light sheet optics. The laser light sheet illuminates the seeding particles. The scattered light of the seeding particles is recorded by the camera at positions downstream from the static mixer. The 200 instantaneous images are analyzed by grayscale normalization to calculate the seeding density. Both, necessary median and median absolute deviation are computed by applying a 13x13 pix filter twice. The conversion factor is chosen to be 1.5 and the minimum noise level is chosen to be  $\frac{1}{4}$  of the bit depth. The S/N ratio for particle threshold is set to 2. The normalized concentration maps at the positions  $1 \cdot Dh$  and  $2 \cdot Dh$  downstream from the static mixer is shown in Figure 10 and Figure 11.

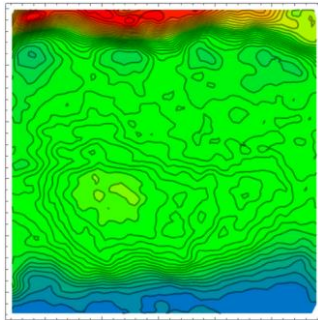


Figure 10 Normalized image concentration at position  $1 \cdot Dh$

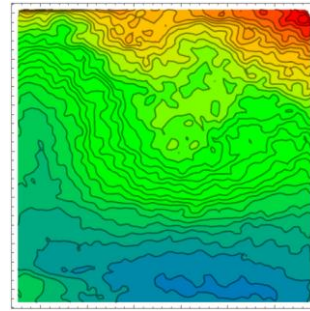
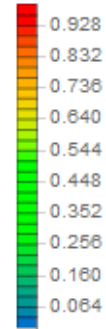


Figure 11 Normalized image concentration at position  $2 \cdot Dh$



## Conclusion and Outlook

The results were post-processed in Wolfram Mathematica and are presented as concentration maps in dimensionless form. The numerical evaluation of mixing effectiveness is expressed as the coefficient of variance  $CoV = \frac{\sigma}{\mu}$  where  $\sigma$  is standard deviation and  $\mu$  is the arithmetic mean of the concentration data. Reynolds number calculated with mean LDA velocity is  $Re = 128\ 000$ . The initial coefficient of variance is  $CoV_0 = 1$ , which is based on concentration measurement without static mixer at the position 1700 mm of the 2<sup>nd</sup> duct. CoV for CFD and physical model are shown in Figure 12. Despite the satisfactory compliance of the data in terms of the CoV between the CFD and image based measurement, there can be visually observed the discrepancy in the concentration maps. This can be explained by the shortcoming in the boundary condition definition. Our boundary condition for the CFD considers only the proper streamwise component of velocity. The definition of the boundary condition can be extended by other components of the velocity, turbulence intensity, swirl, and the concentration distribution of the seeding particles. In further studies we will try to consider these components of boundary conditions as well, which will lead to better compliance between the CFD and image based measurements.

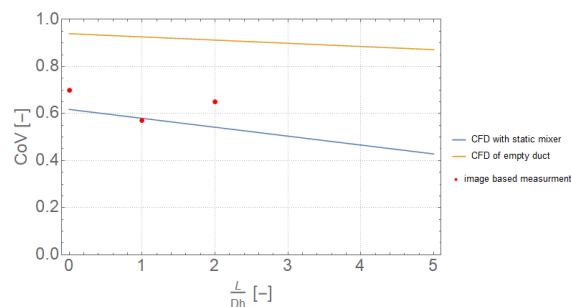


Figure 12 Coefficient of variance of various models along dimensionless length

## References

- [1] Moruz L., Kitzhofer J., Dinulescu M., (2017), Waset Journal, *Experimental investigation of plane jets exiting five parallel channels with large aspect ratio*, 11(4), 801 - 808
- [2] Paul E.L., Atiemo-Obeng V.A., Kresta S.M., (2004), Handbook of Industrial Mixing
- [3] Ghahremanian S., (2014), PhD. Thesis, *A near-field study of multiple interacting jets: Confluent jets*, Linköping University, Institute of Technology, Sweden
- [4] Kresta S.M., Etchells A.W., Atiemo-Obeng V.A., Dickey D.S., (2016), *Advances in Industrial Mixing: A Companion to the Handbook of Industrial Mixing*